

Development of hydrodesulfurization catalyst using comparative model feed reactions and quantum chemical studies.

Hiroyuki Nakamura^a, Masaomi Amemiya^a, Ryutaro Koide^a, Emiel J. M Hensen^b,
Rutger A. van Santen^b, Katsuaki Ishida^a

^a Japan Energy Corporation, 3-17-35, Niizo-Minami, Toda, SAITAMA, 335-8502, Japan

^b Eindhoven University of Technology, Eindhoven, 5600 MB, The Netherlands

ABSTRACT

Model hydrodesulfurization (HDS) catalysts (Ni_{2.75}W₂₁, Co_{2.75}Mo₁₁, Ni_{2.75}Mo₁₁ and Ni_{0.9}Co_{1.85}Mo₁₁ wt% / γ -Al₂O₃) were used in the HDS of dibenzothiophene (DBT) and 4,6-dimethyldibenzothiophene (4,6-DMDBT), with and without addition of H₂S or NH₃.

The NiCoMo catalyst exhibited the highest HDS performance with the additives, while NiMo was the best catalyst without the additives. A comparison of the HDS reaction mechanism via hydrogenation (HYD) and the direct desulfurization (DDS) rate constants among these catalysts showed that the ranking of HYD and DDS rate constants depended on the catalyst and the additives. The behavior of NiW was very similar to NiMo. The total rate constants (HYD + DDS) of NiCoMo were the sums of higher HYD and DDS between the NiMo and CoMo. These results showed that the NiCoMo had two kinds of active sites, similar to NiMo and CoMo.

Quantum chemical studies were applied to study the inhibitions of the additives on NiW, CoMo and NiMo metal edge surfaces. The active site structure of NiW was similar to that of NiMo. The ranking of the adsorption energies of the additives on each surface was in good agreement with experiments.

The ideas derived from these model feed reactions in combination with quantum chemical studies contributed to the development of novel improved catalysts which played an integral part in our new HDS process.

1. INTRODUCTION

The development of highly active hydrotreating catalysts is important issue to satisfy the further tightening of diesel fuel sulfur regulation in worldwide.

Therefore, much attention is given to developing effective technologies to produce ultra-low sulfur diesel fuel, particularly sulfur-free (S = 10 ppmw or less) diesel fuel production. In deep HDS, employed to accomplish this goal, the most refractory sulfur compounds in gas oil are alkyl-dibenzothiophenes with alkyl groups near the sulfur atom (in positions 4 and 6)^{1,2)}. The other problem is inhibition by H₂S^{3,4)} and nitrogen compounds including NH₃^{5,6)}. These inhibitors are generated during HDS and hydrodenitrogenation (HDN) reactions. Their concentration is higher under the conditions of deep HDS.

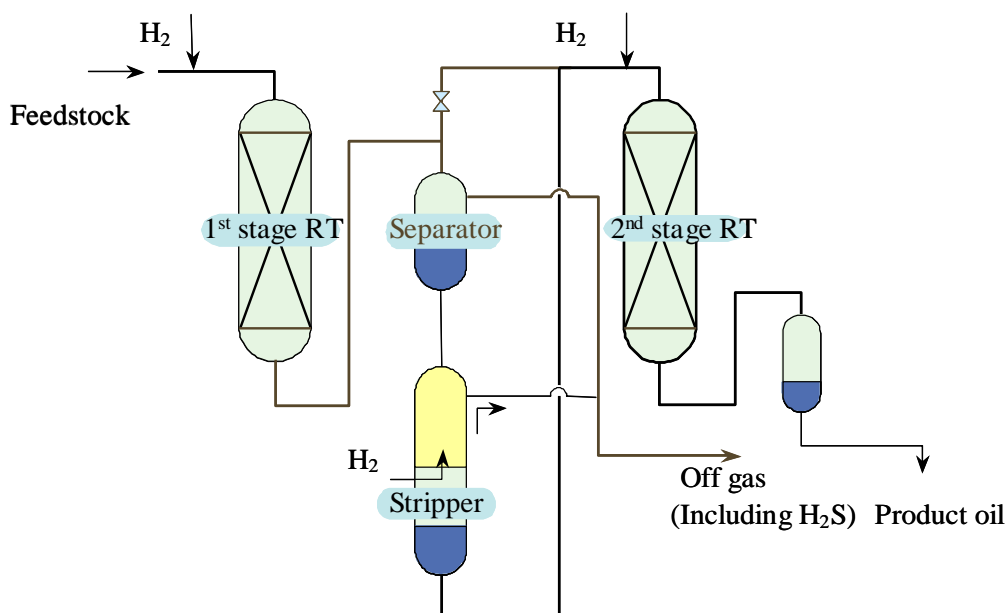


Fig. 1 Pilot plant configuration of the gas liquid separation process (GLSP).

A solution for sulfur-free diesel fuel production, called a two-stage process with gas/liquid separation (GLSP) in between, has been developed by Japan Energy Corporation⁷⁾. This process has a great potential for producing sulfur-free diesel fuel. Removal of produced H₂S and NH₃ in between reactors accelerates HDS in the second-stage reactor here described in Fig. 1. Typical straight gas oil derived from Middle East heavy oil contains 1.2 wt% sulfur and 300 ppmw nitrogen compounds. During ultra-deep HDS operations, the first reactor converts 80-90% of the nitrogen compounds to NH₃ as well as 80-90% of sulfur compounds to H₂S. The authors will examine the inhibition effect of these substances on ultra-deep HDS in the second reactor.

To select or develop the best catalysts for the GLSP system, the promoter effects of Mo and W catalyst were examined, special attention being paid to the inhibition of NH₃ and H₂S. The Ni-, Co- and NiCo-promoted Mo catalysts and the NiW catalyst were prepared by pore-volume impregnation, whilst keeping the support constant. In this way, we were able to clearly understand the inhibition effect of NH₃ and H₂S on the HDS catalysts in conversion of DBT and 4,6-DMDBT.

Moreover, the surface structures of the promoted NiMo, CoMo and NiW catalysts and the corresponding adsorption energies of NH₃ and H₂S on these surfaces were investigated using periodical DFT (density functional theory) calculations. These calculations have been applied to the energetics and structural studies and show good agreement with the experimental data^{8,9)}. In the following, the energetics and structures of the model surfaces adsorbed by NH₃ and H₂S are discussed and compared with the results of the model feed test reactions.

The ideas derived from these model feed reactions in combination with quantum chemical studies contributed to the development of new catalysts, including the catalysts for the GLSP system.

2. EXPERIMENTAL

2.1. Model Catalyst preparation

Catalysts were prepared by pore filling impregnations of γ -Al₂O₃ (pore volume: 0.78cc/g, specific surface area: 380m²g⁻¹) with an aqueous solution of MoO₃, phosphoric acid and Ni carbonate and/or Co carbonate. The catalysts contained 11 wt% Mo and 2.75 wt% Co or 2.75 wt% Ni, or 1.85 wt% Co + 0.9 wt% Ni. The NiW catalysts contained 21 wt% W and 2.75 wt% Ni was prepared by a similar method, as described above, with an aqueous solution of ammoniummetatungstate, phosphoric acid and nickel carbonate. Subsequently, the catalysts were dried in an oven at 393 K for 15 h and finally calcined at 773 K for 30 min.

2.2. Model feed reaction procedures

A sample of 0.5 g of each catalyst was diluted with 9 cm³ α -Al₂O₃ to achieve continuous up-flow in a fixed bed reactor, thereby preventing incomplete catalyst wetting and bypass flow. The model feed consisted of a solution of either 0.20 wt% of 4,6-DMDBT (300 ppmw sulfur) or 0.58 wt% of DBT (1000 ppmw sulfur) in a decaline solution. The amount of the sulfur compounds was measured in the inlet of the second reactor (Fig. 1) incorporating gas/liquid separation. The effect of H₂S on the catalyst performance was tested by addition of 0.05 wt% of a H₂S-generating compound (dimethyldisulfide, DMDS, 10,000 ppmw of H₂S). To explore the effect of NH₃ on the catalyst activity in the HDS of 4,6-DMDBT and DBT, 0.13 wt% of a NH₃-generating compound (tri n-butyl amine, TBA, 300 ppmw of NH₃) was added to the reactant mixture. The catalysts were pre-sulfided in situ with a decaline solution of 2 wt% DMDS at 5.0 MPa and 573 K for 8 hours. The catalysts were tested at 563-603 K at a total pressure of 5.0 MPa, a weight hourly space velocity (WHSV) of 30 hr⁻¹, under 6L hr⁻¹ hydrogen flow for 4,6-DMDBT reactions. For the reactions of DBT, the catalysts were tested at 583-623 K at a total pressure of 5.0 MPa, WHSV of 60 hr⁻¹ under 6 L hr⁻¹ hydrogen flow.

2.3. Catalyst Activity and Reaction Pathways

From the product distributions, the HDS activity was estimated and divided two parts, DDS activity (k_D) and HYD activity (k_H). The reaction products were quantitatively analyzed by gas chromatography. The detailed procedure was referred elsewhere¹⁰. We estimated the first order reaction rate constant for the conversion of DBT and 4,6-DMDBT (k_{HDS}) is the summation of the DDS route (k_D) and the HYD route (k_H), k_D and k_H being defined as follows,

$$k_D = (\text{DDS selectivity}) \times k_{HDS} \quad (1)$$

$$k_H = (\text{HYD selectivity}) \times k_{HDS} \quad (2)$$

$$k_{HDS} = k_D + k_H \quad (3)$$

2.4. DFT Calculations

For our calculations, we have used the Vienna Ab Initio Simulation Program (VASP)¹¹ based on the density functional theory¹². The calculation parameters were similar to those in previous calculations^{13,14}.

The supercell used in the present study was shown in Fig. 2. It contained two Mo(W)S₂ layers

along the x direction (stacking), three Mo (or W) rows along the y direction, and three rows along the z direction. In this axis system, the (100) MoS₂ active surface was represented by the upper layers parallel to the xy plane, and it exhibits alternative rows of exposed molybdenum atoms and sulfur atoms which were commonly called metal edges (or Mo / W edges) and sulfur edges (or S edges).

To determine the most stable sulfur coverage and the structure of the metallic edges before exploring the promoted surface, we have followed the same approach as Cristol¹⁵⁾ by considering the thermodynamic equilibrium of these surfaces with H₂S and H₂ in the gas phase.

The adsorption energy (ΔE_{ADS}) was calculated from

$$\Delta E_{\text{ADS}} = E(\text{S-A}) - E(\text{S}) - E(\text{A}) \quad (4)$$

with $E(\text{S-A})$ being the total energy of surface structure with adsorbent, $E(\text{S})$ the total energy of surface structure and $E(\text{A})$ the total energy of the adsorbent.

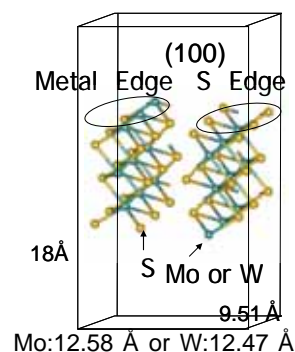


Fig. 2 Representation of the supercell used for calculations.

3. RESULTS

3.1. Model feed experiments

The rate constant divided into k_{H} and k_{D} components for each catalyst for the conversion of 4,6-DMDBT or DBT are shown in Table 1. The HYD route (k_{H}) was dominant ($k_{\text{H}} \gg k_{\text{D}}$) in all the test results of 4,6-DMDBT, while the DDS route was dominant ($k_{\text{H}} \ll k_{\text{D}}$) in all the test results of DBT. The HYD selectivities of NiMo and NiCoMo catalysts are higher than that of CoMo.

Table 1 A list of the average rate constants for the conversion of 4,6-DMDBT and DBT divided into k_{H} and k_{D} .

	k for 4,6-DMDBT ($k_{\text{H}}/k_{\text{D}}$), hr ⁻¹ g ⁻¹				k for DBT ($k_{\text{H}}/k_{\text{D}}$), hr ⁻¹ g ⁻¹			
	NiW	NiCoMo	NiMo	CoMo	NiW	NiCoMo	NiMo	CoMo
BLANK	27.1/3.5	23.9/6.2	52.9/4.7	20.8/7.8	26.9/32.3	23.7/88.8	37.0/59.0	14.2/81.8
+H ₂ S	28.7/8.5	32.7/11.9	40.0/10.2	29.1/8.2	15.1/18.3	22.3/73.5	21.8/29.2	14.4/58.2
+NH ₃	37.3/4.9	30.8/8.9	45.0/6.8	13.5/8.2	18.4/46.7	22.4/94.1	36.1/79.8	13.7/76.1

We observed the differences resulting from different routes among the catalysts, and found that the degree of inhibition by H₂S and NH₃ differ according to the dominant reaction route. The reason for these differences will be discussed in the following section.

NiMo was by far the most active catalyst in a standard 4,6-DMDBT HDS test (a BLANK test). The ratio of the first order reaction rate constant of NiMo in the presence of H₂S to that of the blank test strongly decreased. The first order reaction rates of other catalysts also decreased in the presence

of H₂S.

The presence of NH₃ significantly decreased the overall reaction rate constant for the conversion of 4,6-DMDBT for all tested catalysts to a great extent. Interestingly, the reaction rate constant of CoMo catalyst decreased more significantly with addition of NH₃. The rate constant of NiCoMo catalyst in the blank test for HDS of DBT was slightly higher than those of the other catalysts, the rate constants of the catalysts being almost the same except compared to NiW.

The presence of H₂S significantly decreased the overall reaction rate constant for the conversion of DBT for all tested catalysts to a greater extent than that for the blank test. NiCoMo was the most active catalyst for the conversion of DBT in the presence of H₂S. The presence of NH₃ significantly decreased the activity of CoMo; the rate constants of the other catalysts were not decreased by NH₃ as much. Especially, HYD route rate constants of NiMo and NiW for 4,6-DMDBT were higher than those with H₂S and HYD route rate constants of NiW and NiCoMo were even higher than those of the blank test.

3.2. Inhibiting effect of NH₃ and H₂S by DFT calculations

We have built the most stable promoted MoS₂ and WS₂ surfaces by substituting Mo or W atoms to Ni or Co atoms of these edges and found that a S atom binds to a W atom directly atop while the Ni atom remained uncovered. In contrast the Co atom shared a bridged S atom with a W atom (Fig. 3). This particular structure of the NiW was also described by Sun et al.¹⁶. The bond lengths of each S bridge between the promoted metal and Mo or W are a function of binding energy between S atom and metal atoms.

The ranking of binding energy was as follows, Ni-S(92)<Co-S(113)<<Mo-S(167)<W-S(175 kJ mol⁻¹)

The bond length of 'a' (See Fig. 3) in each catalyst is as follows,

$$\text{CoMo}(2.22) < \text{CoW}(2.31) < \text{NiMo}(2.39) < \text{NiW}(4.14 \text{ \AA})$$

The bond length of 'b' (See Fig. 3) in each catalyst is as follows,

$$\text{CoMo}(2.34), \text{CoW}(2.35), \text{NiMo}(2.34) \gg \text{NiW}(2.16 \text{ \AA})$$

When the S-Ni (or Co) binding energy is weaker than the S-Mo (or W), the length of 'a' should be higher than 'b'. If the difference of the energy is much more, the sulfur atom binds to a tungsten or molybdenum atom directly atop. That is the reason why NiW forms the particular structure.

Finally we have calculated adsorption energy of H₂S and NH₃ on CoMo, NiMo, and NiW catalysts by VASP and compared to the experimental results.

The rankings of adsorption energy of NH₃ or H₂S were as follows,

$$\text{H}_2\text{S}: \text{NiW}(79.1) > \text{CoMo}(56.7) > \text{NiMo}(13.7 \text{ kJ mol}^{-1})$$

$$\text{NH}_3: \text{CoMo}(112.9) > \text{NiW}(88.8) > \text{NiMo}(70 \text{ kJ mol}^{-1})$$

These orders of inhibitions were good agreement with the experimental results except the

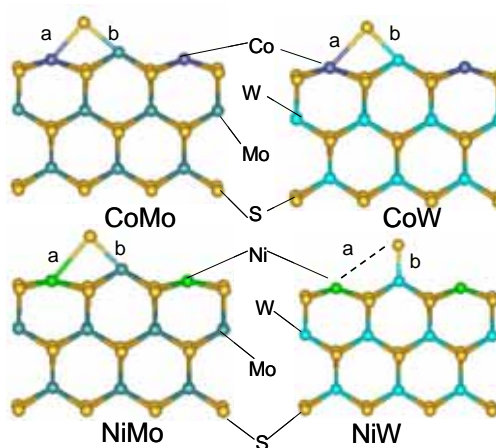


Fig. 3 Comparison between the promoted MoS₂ and WS₂ catalyst surface structures.

adsorption energy of H₂S on the CoMo catalyst. The reason for this exception will be discussed in the following section.

4. DISCUSSION

4.1 Inhibition effect of H₂S and NH₃ on HYD and DDS reaction pathways

In an attempt to identify the active site of the promoted catalysts, we determined which route was poisoned by H₂S and NH₃ by comparing separately values for k_H and k_D of the blank test with those of tests with H₂S- and NH₃-containing feeds.

Fig. 4 showed the average inhibition degree of k_H and k_D for the conversion of 4,6-DMDBT as compared to blank tests performed at the same temperature in the presence of H₂S and in the presence of NH₃.

The inhibition of H₂S in the HYD route on NiMo catalyst was clearly shown. The CoMo catalyst was weakly poisoned by H₂S. Poisoning for NiCoMo was moderate and intermediate between that of NiMo and CoMo. On the other hand, the DDS route of CoMo and NiCoMo were strongly poisoned by H₂S. This implies H₂S was adsorbed on the active site of DDS. The inhibition effect of H₂S and NH₃ was more evident for 4,6-DMDBT HDS than for HDS of DBT. The sulfur atom in 4,6-DMDBT was difficult to remove because of the steric hindrance of the methyl groups¹⁷⁾. The reaction route for HDS of 4,6-DMDBT usually followed a HYD route. Therefore, this is a reasonable explanation for the difference in inhibition compared to HDS of DBT.

The role of H₂S on hydrotreating sulfide catalysts has been studied extensively in the literature. Texier et al.¹⁸⁾ reported that the addition of H₂S increased the HDS activity. Reinhoudt et al.⁵⁾ also reported that the addition of H₂S increased catalytic activity of CoMo in the HDS for 4,6-alkylated DBT and DBT. In our study, we did not observe such an increase. However, the high tolerance to H₂S poisoning of NiCoMo and CoMo could follow the same mechanism as the earlier reported increase in activity. The adsorption of H₂S on the CoMo surface may form a HYD active site.

In our previous study¹³⁾, the mobility of hydrogen on various CoMo sulfide surfaces has been studied. We found that a CoMo catalyst could form various types of adsorbed sulfur atoms which

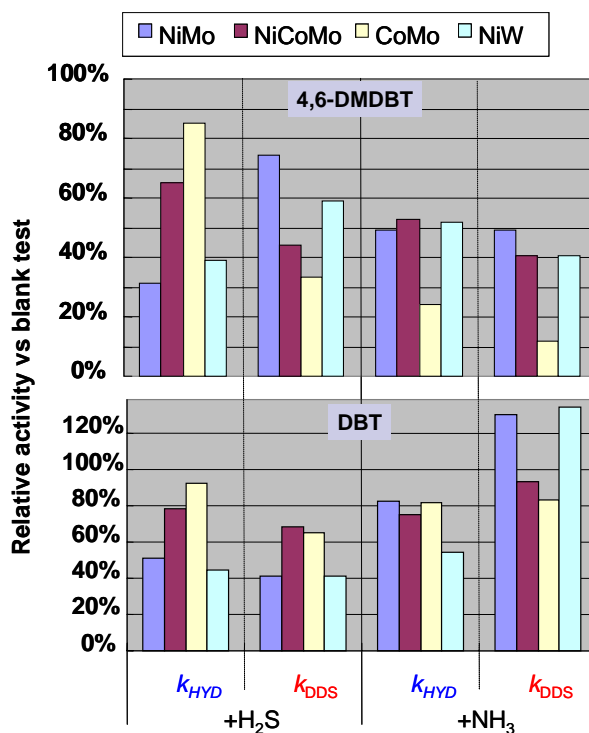


Fig. 4 Inhibition effect of H₂S and NH₃ on k_H and k_D of 4,6 DM-DBT and DBT for each catalyst.

can easily dissociate hydrogen molecules. Therefore, a CoMo catalyst can show a high tolerance to H₂S despite the high adsorption energy.

The inhibition effect of NH₃ was also exemplified in Fig. 4. NH₃ poisoned strongly both the HYD and DDS active site on CoMo catalyst both for DBT and 4,6-DMDBT HDS. In case of 4,6-DMDBT, NiCoMo catalyst behaved much like NiMo catalyst concerning NH₃ poisoning. In the case of DBT poisoned with NH₃, NiMo catalyst showed a high tolerance for NH₃. Especially, k_D of NiMo catalyst exhibited almost the same activity as the blank test in the case of DBT poisoned with NH₃. The active site of NiW and NiMo should be different from CoMo because the inhibition effect in the model feed experiment was quite different. In our previous study¹³⁾, we found hydrogen was able to break Ni-S bonds in NiMo sulfide surfaces of the S-Ni-S bridge structure. This broken structure was quite similar to the NiW catalyst surface which we have shown in Fig. 3.

For the model feed experiments, there was a very large change in k_D upon addition of H₂S or NH₃. Compared to H₂S adsorption energy calculated by the VASP, the adsorption energy of NH₃ was higher, however, adsorption energy of actual S compounds may be higher than NH₃.

In the NiMo and NiW case, the surface may be protected from H₂S by NH₃.

The ranking of adsorption energy on each catalyst surface was as follows,

NiW: NH₃ (88.8) > H₂S (79.1 kJ mol⁻¹)

NiMo: NH₃ (70) >> H₂S (13.7 kJ mol⁻¹)

CoMo: NH₃ (112.9) >> H₂S (56.7 kJ mol⁻¹)

In the CoMo case, NH₃ may be strongly connected to the surface and completely poison the active site.

4.2 Catalyst for the first reactor of the GLSP system

The NiCoMo catalyst was the best catalyst for HDS of DBT in all cases. After calculating k_H and k_D , we found an interesting result in the sum of k_H and k_D .

The NiCoMo catalyst comprised Ni, Co and Mo impregnated in the same support. On this surface, there were two active sites located together. Examining the inhibition effect of H₂S and NH₃, we found that the nature of NiMo and CoMo catalysts to be quite different. The CoMo catalyst had a high tolerance for H₂S whereas the NiMo catalyst had a high tolerance for NH₃. If there are two different active sites on NiCoMo catalyst, and k_H and k_D are different for NiMo and CoMo, the NiCoMo HDS activity should be the sum of higher values of k_H and k_D .

We highlighted the higher of the values of k_H and k_D for NiMo, CoMo and compared the values of NiCoMo catalyst and calculated value of NiCoMo in Table2.

Although there were some variations at higher temperatures, the activity of NiCoMo catalyst had a good correlation with the sum of the higher values of k_H and k_D for NiMo and for CoMo in the presence of rich H₂S conditions.

The CoMo catalyst had a higher k_D value than the NiMo catalyst while the NiMo catalyst had a higher value of k_H . NiCoMo catalyst activity was a sum of k_D of CoMo and k_H of NiMo. Therefore, the total HDS activity was the highest. It is known that catalytic reactions proceed through the lowest barrier. NiCoMo catalyst had two kinds of active sites, and the reaction pathway proceeded through the active site with the lower barrier.

Table 2 Comparison of k_H and k_D for the conversion of 4,6-DMDBT or DBT with H_2S or NH_3 between the calculated proportional distribution and the NiCoMo catalyst. (k_H and k_D ; $hr^{-1}g^{-1}$)

Feed	Reaction temperature / K	CoMo		NiMo		NiCoMo		calculated*	
		k_H	k_D	k_H	k_D	k_H	k_D	k_H	k_D
+H ₂ S	593	9	36	12	14	12	35	10	29
	603	13	54	18	23	19	55	14	43
	613	17	69	25	34	21	88	20	57
+NH ₃	593	7	44	16	57	9	56	10	48
	603	12	71	27	71	15	75	17	71
	613	16	90	47	93	28	110	26	91

Mesh: Higher k_H and k_D values between CoMo and NiMo.

* The proportional distribution of 66% CoMo and 33% NiMo.

In the presence of NH_3 condition, k_H and k_D of NiCoMo were both higher than those of CoMo while the values were close to the calculated proportional distribution of 66% CoMo and 33% NiMo.

Finally, we found that a NiCoMo catalyst was the best catalyst for the first reactor because NiCoMo had the high tolerance for both H_2S and NH_3 .

4.3 Catalyst for the second reactor of the GLSP system

According to the model feed experiment, NiMo catalyst was the best catalyst for the second reactor because NiMo had high HDS activity under lean H_2S conditions.

However, our DFT studies implied NiW catalyst had the strongest adsorption energy to H_2S . The experiment results showed the NiMo and NiW display similar catalytic behavior, which meant that the active sites should be similar. Actually, the sulfided NiW structure contained bare Ni atoms on the metal edges. NiMo had a similar structure to NiW in case of H_2 adsorption on the active site¹³. It should be mentioned that the model catalyst was prepared at the same molar ratio as the other catalysts without any further optimization. Kishan¹⁹ reported that the key step in the formation of the bare Ni on the WS_2 surface was the order in which Ni and W precursors transfer to the sulfidic state. In NiW systems prepared by conventional methods the sulfidation of Ni precedes that of W.

In order to retard the sulfidation of Ni, we used ethylenediaminetetraacetic acid (EDTA). For EDTA the Ni sulfidation was delayed to temperatures where WS_2 was already formed. This catalyst showed the highest activity in HDS at lean H_2S condition, indicating that completed sulfidation of W preceding that of Ni provided the ideal circumstances for NiWS formation.

4.4 Application to the GLSP system for the developed catalyst

In order to confirm the idea, we have conducted the real feed test using our developed catalyst. Fig. 5 showed the final results of real feed tests²⁰. RUN1 showed our conventional CoMo catalyst which was used for 500 ppm sulfur level.

The difference between RUN1 and RUN3 was the effect of GLSP. RUN5 was to confirm the model feed result for the second reactor. According to the DFT study, NiW had some potential, so we developed the NiWS catalyst which had the ideal surface as mentioned above.

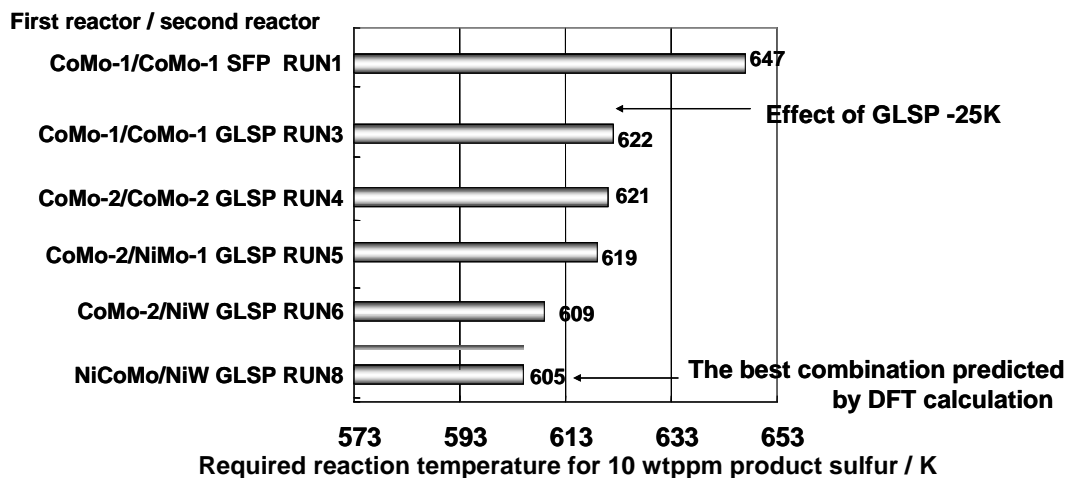


Fig. 5 Evaluation of catalysts combination in the gas liquid separation system reactors.

GLSP: Gas liquid separation process; SFP: Conventional single flow process

RUN1-3: Feed (S=1.69 wt%, N=69 ppmw), $P_{H_2}=5.0$ MPa, $H_2/Oil=200$ NL L^{-1} , $LHSV=2.0$ hr^{-1}

RUN4-8: Feed (S=1.69 wt%, N=104 ppmw), $P_{H_2}=5.0$ MPa, $H_2/Oil=200$ NL L^{-1} , $LHSV=2.0$ hr^{-1}

The result was significant but according to the model feed experiment, NiCoMo catalyst should be the best in rich H_2S condition. Therefore, we selected NiCoMo/NiW as the final combination for GLSP.

Consequently, the selected system showed the best performance in our system and this newly developed system is suitable for obtaining sulfur-free fuel cost effectively.

5. Conclusions

Inhibition effects of NH_3 and H_2S on CoMo, NiMo, NiW and NiCoMo catalyst were studied by model feed experiments and comparative quantum chemical studies. It was demonstrated that the presence of H_2S and NH_3 had a large effect on the catalyst ranking and the relative importance of reaction pathways, i.e. k_H and k_D , for the conversion of both DBT and 4,6-DMDBT. The NiCoMo catalyst exhibited the highest HDS performance with the additives, while NiW was the best catalyst without the additives. A comparison of the HDS reaction mechanism via HYD and DDS rate constants among these catalysts showed that the ranking of HYD and DDS rate constants depends on the catalysts and the additives. The behavior of NiW was very similar to NiMo. The total rate constants (HYD + DDS) of NiCoMo were the sums of higher HYD and DDS between the NiMo and CoMo. These results suggested that the NiCoMo had two kinds of active sites, similar to NiMo and CoMo.

Quantum chemical studies were applied to study the inhibition effect of the additives on NiW, CoMo and NiMo metal edge surfaces. The active site structure of NiW was similar to NiMo, and the ranking of the adsorption energies of the additives on each surface was in good agreement with experiments.

The best combination of the catalysts in the first and the second reactor for the two stage process with the GLSP system was considered to be as follows.

In the first reactor, NiCoMo catalyst was the best catalyst because of the high tolerance for both H₂S and NH₃. In the second reactor, the developed WS₂ catalyst whose metal edge modified by Ni atoms using EDTA precursor was the best catalyst.

This combination decreased the operation temperature by 42 K to maintain sulfur-free fuel oil production compared to the conventional CoMo catalyst for 500 ppmw S production. This corresponded to a twofold higher activity of the catalysts than that of the conventional CoMo catalyst.

Acknowledgement

This study was partially entrusted by the New Energy and Industrial Technology Development Organization.

References

- ¹ M. Houalla, D. Broderick, A. V. Sapre, N. K. Nag, V. J. H. de Beer, B. C. Gates, H. Kwart, *J. Catal.*, 61, 523(1980).
- ² T. Kabe, A. Ishihara, H. Tajima, *Ind. Eng. Chem. Res.*, 31,1577(1992)
- ³ T. Isoda, X. Ma, I. Mochida, *Sekiyu. Gakkaishi*, 37, 506(1994)
- ⁴ Q. Zhang, W. Qian, A. Ishihara, T. Kabe, *Sekiyu. Gakkaishi*, 40, 185(1997)
- ⁵ H. R. Reinhoudt, M. van Gorsel, A. D. van Langeveld, J. A. R. van Veen, S. T. Sie, J. A. Moulijn, *Stad. Surf. Sci and Catal.*, 127, 211 (1999)
- ⁶ V. LaVopa, C.N. Sattterfield, *J. Catal.*, 110, 375(1988)
- ⁷ Japan Energy Corporation, *Registered patent in Japan*, JP4002733(2007)
- ⁸ L.S. Byskov, M. Bollinger, J.K. Norskov, B.S. Clausen, H. Topsøe, *J. Mol. Catal.*, 163, 117(2000)
- ⁹ (a) P. Raybaud, J. Hafner, G. Kresse, S. Kaxztelan, H. Toulhoat, *J. Catal.*, 189, 129(2000)
(b) P. Raybaud, J. Hafner, G. Kresse, H. Toulhoat, *Stad. in Surf. Sci. and Catal.*, 127, 309(1999)
- ¹⁰ H. Nakamura, M. Amemiya, K. Ishida, *J. Japan Petrol. Inst.*, 48, 281(2005)
- ¹¹ (a) G. Kresse, J. Hafner, *J. Phys. Rev. B*, 47, 558(1993); *Phys. Rev. B*, 49, 14221(1994)
(b) G. Kresse, J. Furthmuller, *J. Phys. Rev. B*, 6,15(1996); *Phys. Rev. B*, 54,11169(1996)
(c) <http://cms.mpi.univie.ac.at/vasp/>
- ¹² (a) P. Hohenberg, W. Kohn, *Phys. Rev. B*, 136, 864(1964)
(b) W. Kohn, L.J. Sham, *Phys. Rev. A*, 140, 1133(1965)
- ¹³ A. Travert, H. Nakamura, R.A. van Santen, S. Cristol, J.-F. Paul, E. Payen, *J. Am. Chem. Soc.*, 124, 7084(2002)
- ¹⁴ H. Nakamura, *Ph.D. thesis*, Tohoku University (2004)
- ¹⁵ S. Cristol, J.F. Paul, E. Payen, D. Bougeard, J. Hafner, F. Hutschka, *Stad. in Surf. Sci. and Catal.*, 127, 327(1999)
- ¹⁶ M. Sun, A.E. Nelson, J. Adjaye, *J. Catal.*, 226, 41(2004)
- ¹⁷ T. Isoda, Y. Takase, N. Isumi, K. Kusakabe, S. Morooka, *Sekiyu. Gakkaishi*, 41, 318(1998).
- ¹⁸ S. Texier, G. Berhault, G. Pérot, V. Harlé, F. Diehl, *J. Catal.*, 223, 404(2004).
- ¹⁹ G. Kishan, L. Coulier, V.H.J. de Beer, J.A.R. van Veen, J.W. Niemantsverdriet, *J. Catal.*, 196, 180(2000)
- ²⁰ Petroleum Energy Center, The final report on the development of pollutant reduction technologies in petroleum, 152-238(2004), <http://www.nedo.go.jp/database/index.html>, Barcode No.10000260820